

A Novel Fusion Antibody Exhibits Antiangiogenic Activity and Stimulates NK Cell-mediated Immune Surveillance Through Fused NKG2D Ligand

Desmond O. Acheampong,* Mingying Tang,* Youfu Wang,* Xin Zhao,*
Wei Xie,* Zhiguo Chen,* Wenzhi Tian,† Min Wang,* and Juan Zhang*

Summary: A single-chain variable fragment (scFv) targeting vascular endothelial growth factor receptor 2 was previously generated from a phage display library in our laboratory. However, it has shortened half-life and lacks Fc fragment for effector cell recognition. To address these challenges, a ligand of NK-cell receptor NKG2D was fused to the scFv and created a fusion protein scFv-major histocompatibility complex class I-related chain A (MICA), which is expected to recognize tumor cells through the scFv moiety and stimulate NK cells through the MICA. The fusion protein demonstrated specific binding to both vascular endothelial growth factor receptor 2 and NKG2D in protein-based and cell-based assays. In addition, it demonstrated antiangiogenic activities including restraining the proliferation, migration, transwell invasion, and tube formation of human umbilical vein endothelial cells. Furthermore, the fusion protein exhibited significant cytotoxicity on K562, MDA-MB-435, and B16F10 cells and triggered NK92 cell-mediated cytotoxicity on MDA-MB-435 cells by stimulating the release of significant cytokines. The fusion protein targeting strategy, therefore, provides a means to engage lymphocyte effector cells against tumor specific antigen overexpressing tumor cells.

Key Words: antiangiogenesis, NKG2D, fusion protein, scFv-MICA, antibodies

(*J Immunother* 2017;40:94–103)

Vascular endothelial growth factor and its receptor (VEGF/VEGFR2) targeted antiangiogenic therapy is arguably a preferred strategy for tumor elimination nowadays.¹ Both small molecular receptor tyrosine kinase inhibitors and monoclonal antibodies (mAbs) have proved effective in cancer therapy, among which bevacizumab (avastin) and ramucirumab (cyramza) are clinically defined mAbs. Notwithstanding, Ramucirumab has the potential to cause serious side effects such as hemorrhage, hypertension, and diarrhea.² Fatal conditions such as proteinuria and gastrointestinal perforation have also been reported on ramucirumab treatment.² These side effects are presumably attributed to its off-target binding by the Fc moiety and the large molecular size. Like other mAbs, <20% of the administered dose gets to the tumor microenvironment due to large molecular size.^{3,4} We previously generated an anti-

VEGFR2 single-chain variable fragment (scFv) AK404R from a human antibody phage display library⁵ which exhibited high affinity for VEGFR2 and potent antiangiogenic activity. However, it has shortened half-life coupled with the fact that it lacks Fc fragment for effector cell recognition. To address these challenges, in this study we aimed at fusing major histocompatibility complex class I-related chain A (MICA) to the scFv and creating a fusion protein (scFv-MICA). The fusion protein has molecular size of 70 kD, which is approximately twice the molecular size of a scFv, and half the size of a full-length antibody. The MICA moiety is one of the stress-inducible ligands of natural killer group 2D (NKG2D), a homodimeric C-type lectin-like receptor of natural killer cells (NK), T cells, and natural killer T cells.^{6–8} The NKG2D/MICA system, therefore, provides a specific system for immune cells to recognize tumor cells and the tumor microenvironment. Because most tumor cells over express VEGFR2,^{9–15} the fusion protein targeting, provides a means to engage effector cells against different kinds of VEGFR2 positive tumor cells.

MATERIALS AND METHODS

Cell Culture

The adherent human umbilical vein endothelial cells (HUVECs) were cultured in endothelial culture medium (ECM) supplemented with fetal bovine serum (FBS) and endothelial cell growth supplement. Human embryonic kidney cell line HEK293 was cultured in Dulbecco's Modified Eagle Medium (high glucose), supplemented with FBS. Human leukemic cell lines U937 and K562 and B16F10 were cultured in RPMI 1640 medium, supplemented with FBS. MDA-MB-435 cells were cultured in Dulbecco's Modified Eagle Medium (high glucose) with FBS. NK92 was cultured in RPMI 1640 medium, supplemented with 0.2 mM inositol, 0.1 mM 2-mercaptoethanol, 0.02 mM folic acid, 200 U/mL recombinant IL-2, 12.5% horse serum, and 12.5% FBS. Cell culture media and supplements were purchased from Life technologies (Basel, Switzerland). HUVECs were purchased from Beijing Yu Heng Technology Co., Ltd, Beijing, China. Other cell lines were preserved in our lab.

Plasmid Construction of Fusion Protein scFv-MICA

PCR mastermix was purchased from Biotek (Beijing, China). Restriction and modification enzymes were purchased from Takara (Otsu, Japan) and NEB (New England Biolabs). Vector pPICZ α , *Pichia pastoris* (strain X-33) and *Escherichia coli* (strain DH5 α) were obtained from Invitrogen life technologies. Full-length anti-VEGFR2 scFv

Received for publication July 1, 2016; accepted January 4, 2017.
From the *State Key Laboratory of Natural Medicines, School of Life Science & Technology, China Pharmaceutical University, Nanjing; and †ImmuneOnco BiopharmCo., Ltd, Shanghai, P.R. China.
D.O.A., M.T., and Y.W. contributed equally.
Reprints: Juan Zhang, State Key Laboratory of Natural Medicines, China Pharmaceutical University, 154#, Tongjiangxiang 24, Nanjing 210009, P.R. China (e-mail: juancpu@126.com).
Copyright © 2017 Wolters Kluwer Health, Inc. All rights reserved.

was amplified using pHEN2-anti-VEGFR2 scFv as template, with Primer 1 and Primer 2 being (5'GGAA TTCGAGGTGCAGCTGGTG3') and (5'GGTTCTGAAC CACCACCACCTAGGACGGTCAG 3'), respectively. Secondly, MICA was amplified, using pET28a-MICA as template, with Primer 3 and Primer 4 being (5'TAGGTGGTGGTGGTGGTTTCAGAACCTCACAGC CTG3') and (5'GCTCTAGAGCTCAATGATGATGATG ATGATGCTTGCCGCTTGGGAC3'), respectively. The fusion gene scFv-MICA was then created by joining the anti-VEGFR2 scFv to the extracellular domain of human MICA (residues 1-276; accession numbers-MICA: Q29983.1) with a G₄S linker. Finally, a histidine tag (6 × His) was added to the C-terminus of MICA to facilitate purification of the fusion protein. Subsequently, the fusion gene was sub-cloned into pPICZ α (restriction sites *EcoRI* and *XbaI*). Afterwards, DH5 α was transformed with the recombinant vector pPICZ α -scFv-MICA and grown on Luria-Bertani plate containing zeocin at 37°C for 16–24 hours.

Transfection of *P. pastoris*

The recombinant vector pPICZ α -scFv-MICA was then extracted from the transformed DH5 α and linearized, using *BstXI* (New England Biolabs). *P. pastoris* (strain X-33) was then transformed with the linearized pPICZ α -scFv-MICA by electroporation, using an ice cold 0.2 cm electroporation cuvette (V: 1500, μ F: 25). The transformed *P. pastoris* was then grown on yeast extract peptone dextrose plates containing zeocin at 30°C for 1–3 days to select the clones which were successfully transformed.

Expression and Purification

To select the clone with the highest target protein expression, protein expression levels of 50 positive clones were screened by sodium dodecyl sulfate polyacrylamide gel electrophoresis (SDS-PAGE) and Western blot. The highest protein expression clone selected was then grown in yeast extract peptone dextrose liquid medium (100 μ g/mL zeocin) at 30°C and shaking at 220 rpm overnight to an OD₆₀₀ of 2–4. It was then subcultured in BMGY medium (buffered glycerol complex medium) containing 0.5% glycerol at 30°C and shaking at 220 rpm overnight. Subsequently, it was centrifuged (3000g, 5 min) to collect the cell pellet. The cell pellet was then suspended to an OD₆₀₀ of 1.0 in BMMY medium (buffered methanol complex medium) with 0.5% methanol and grown to induce expression. Sterilized pure methanol was added to a final concentration of 0.5% methanol every 24 hours to maintain induction for additional 4 days. Finally, the culture was centrifuged to collect the secreted fusion protein. Subsequently, the target protein was purified by nickel column chromatography. The purity level was evaluated by SDS-PAGE, Western blot, and size exclusion chromatography.

Size Exclusion Chromatography (SEC) and Immunoblotting

SEC analysis was performed on an Agilent 1200 Series (Agilent Corp., Santa Clara, CA), high performance liquid chromatography system equipped with a binary pump, micro degasser, an autosampler, and a thermostatically controlled column compartment. The wavelength of 278 nm was chosen as the appropriate wavelength for detection on the UV detector. The flow rate was 0.7 mL/min under isocratic condition and 20 μ L of the protein (1 mg/mL)

injected into the high performance liquid chromatography system.

NKG2D/KDR3 (the extracellular domain 3 of human VEGFR2) and scFv (control) were loaded into 15% (w/v) SDS-PAGE gel for electrophoresis and transferred onto polyvinylidene difluoride membrane (Millipore). It was then incubated with MICA mAb (1:2000, Mouse, Code: K0217-3, Clone: AMO1, Concentration: 1 mg/mL, Medical & Biological Laboratories Co., Ltd) at 37°C for 2 hours. It was then washed with phosphate buffer saline (PBS) and incubated with horse radish peroxidase (HRP)-conjugated goat anti-mouse IgG (1:5000, Millipore) at 37°C for 1.5 hours. Finally, the blots were treated with enhanced chemiluminescence solution and exposed in gel imaging system (Bio-Rad). KDR3, MICA, and NKG2D were expressed and purified in our laboratory.¹⁶

Quantitative Enzyme-linked Immunosorbent Assay

Two 96-well plates were coated with either 1000 nM NKG2D or 1000 nM KDR3 diluted in plating buffer (0.05M NaHCO₃, pH 9.6), and incubated at 4°C overnight. Subsequently, the wells were blocked with PBS containing 5% skim milk and incubated at 37°C for 2 hours. Afterward, they were incubated with serial dilutions (from 0.5 to 1000 nM) of the fusion protein at room temperature (RT) for 1.5 hours. The NKG2D/KDR3-plated wells which were not treated with the fusion protein were used as control. The plates were incubated with MICA mAb (1:2000) diluted in 3% skim milk at RT for 1.5 hours. Subsequently, they were incubated with HRP-conjugated goat anti-mouse IgG (1:5000, Millipore) at RT for 1.5 hours. Finally, 3,3',5,5'-tetramethylbenzidine peroxidase substrate (bovine serum albumin) was added followed by 50 μ L of 2.5 M sulfuric acid to stop the enzyme action. The absorbance was measured at OD₄₅₀–OD₆₃₀.

Binding Kinetics of Fusion Protein

The binding kinetics of the fusion protein against KDR3 and NKG2D were measured with a Biacore X100 instrument (Biacore X100, GE Healthcare, Sweden) at 25°C. Firstly, the running buffer and the dispenser buffer were filtered and degassed prior to the study. The fusion protein was subsequently diluted in the running buffer and immobilized on Sensor Chip CM5 (GE Healthcare, BR-1000-12) with target resonance unit density of 2000. Different concentrations of KDR3 (250, 125, 62.5, 31.5, 15.6, 7.8 nM)/NKG2D (250, 125, 62.5, 31.5, 15.6, 7.8 nM) were then injected and capture done at a constant flow rate of 40 μ L/min. Sensorgrams were obtained at each concentration and evaluated by the BIA Evaluation 2.0 program. The kinetic constants association (k_a), dissociation (k_d), and equilibrium constant K_D were then calculated with 1:1 binding model.

RNA Silencing and Plasmids Construction

Specific NKG2D (GenBank accession number AJ001687.1) shRNA (5' GGATCCCGGATGGGACTAG TACACATTCTTCAAGAGAGAATGTGTACTAGTCCC ATCCTTTTTTCCAAGAATTC3') sequences were designed, produced, and cloned into pLVX-shRNA vector. The plasmids were transfected into HEK293T by Lipofectamine 2000 (Invitrogen) according to manufacturer's instructions. Lentiviral plasmids supernatant production was then collected after 24 hours and 48 hours incubation respectively at 37°C.

Subsequently, NK92 cells were transiently transfected with lentiviral plasmids pLVX-shRNA-NKG2D by Lipofectamine 2000 and incubated at 37°C for 72 hours.

Flow Cytometry Assay

Flow cytometry assays were conducted to evaluate the binding of fusion proteins to HUVEC, U937, and HEK293 cells. In total, 5×10^5 of HUVEC, U937, and HEK293 cells per sample were suspended in PBS containing 5% bovine serum albumin and incubated with 2000 nM of fusion protein at 4°C for 1 hour. The cells were then incubated with His-probe (H-15) rabbit (sc-803) or goat (sc-803-G) polyclonal affinity-purified antibody (Santa Cruz Biotechnology). The cells were subsequently washed and binding assays performed with a BD FACS flow cytometer. MICA, scFv, and PBS were used as controls.

Cell Proliferation Assay

HUVECs or HEK293 cells (4×10^3 cells/well) were seeded into 96-well plate and incubated at 37°C for 24 hours and treated with serial diluted proteins (from 0 to 500 nM). The fusion protein were then added to the wells and incubated at 37°C for 24, 48, or 72 hours. The untreated groups were used as vehicle of control. Subsequent to incubation, cell viability, was quantified by 3-(4,5-Dimethylthiazol-2-yl)-2,5-diphenyltetrazolium bromide (MTT) assay, and the inhibitory rates expressed as percentages for the vehicle control (100%). Thus, MTT solution was added to each well and incubated at 37°C for 4 hours. This was followed by the addition of dimethyl sulfoxide to each well for formazan solubilization. Finally, the optical density of each well was measured at 570 and 630 nm by a microplate reader (Thermo), and the inhibitory rate calculated using the formula: Inhibitory rate (%) = (mean control absorbance - mean experimental absorbance) / (mean control absorbance) \times 100. The IC₅₀ values were then calculated with curve fitting. MICA, scFv, and PBS were used as controls.

Wound Healing Assay

HUVECs of concentration 2×10^5 cells/well were seeded into a 12-well plate. The cells were starved for 12 hours then scratched with a 1 mL pipette tip. It was subsequently incubated with different concentrations of the fusion protein (0, 20, 100, and 500 nM) for 0, 12, 16, 20, or 24 hours. The resultant images were then captured with OLYMPUS fluorescence microscope in the same field at 0, 12, 16, 20, and 24 hours, respectively. The wound healing ability of the fusion protein was defined by the ratios of the decreased scratch width after 12, 16, 20, and 24 hours, respectively, relative to the initial scratch width in the same field, and calculated as follows: Rate of wound healing (%) = $100 \times$ (the initial scratch width - the scratch width of corresponding time point) / the initial scratch width. MICA, scFv, and PBS were used as controls.

Transwell Invasion Assay

HUVEC cells (1×10^4) were mixed with different concentrations of the fusion protein (20, 100, and 500 nM) and suspended in serum-free medium. They were then added to the top 24 transwell chambers coated with Matrigel (Millipore, Billerica, MA). Afterward, the bottom chambers were filled with ECM and endothelial cell growth supplements, and then incubated for 12 hours. Subsequent to that, noninvasive cells on the top surface of the membrane were removed with cotton swabs and the invaded

cells fixed with 4% polyoxymethylene for 20 minutes and washed. The cells were then stained with crystalline violet. Images were then captured with an OLYMPUS inverted microscope at $\times 100$ magnification, and the cells counted with Image-pro-plus program. Invasion percentages were quantified on the basis of untreated sample (control). MICA, scFv, and PBS were used as controls.

Tube Formation Assay

Matrigel (BD Biosciences) were thawed on ice for 24 hours and then aliquots per well were coated on a 96-well tissue culture plate and incubated at 37°C for 1 hour to solidify. 1×10^4 HUVEC cells were then seeded into the 96-well plate, and was followed by the addition of ECM supplemented with 1% (v/v) endothelial cell growth supplements. It was subsequently incubated with different concentrations of the fusion protein (0, 20, 100, and 500 nM) for 8 hours. Afterward, endothelial tube formation was photographed with an inverted OLYMPUS microscope at $\times 100$ magnification and counted with image-pro-plus program. The experiments were independently performed at least 3 times. MICA, scFv, and PBS were used as controls.

Western Blot Analysis

2×10^5 HUVECs were seeded into a 6-well plate and the whole cell extracts harvested. Proteins were then resolved by electrophoresis then transferred onto polyvinylidenedifluoride membranes and subsequently incubated with primary antibodies anti- β -actin (Anbo), anti-protein kinase B (AKT) (Cell Signaling) and anti-P38 mitogen-activated protein kinases (MAPK) (Anbo), and phospho-specific anti-AKT (Ser⁴⁷³) (EPITOMICS, Burlingame, CA) and anti-P38 MAPK (Thr¹⁸⁰/Tyr¹⁸²) (Cell Signaling). They were then incubated with HRP-conjugated goat anti-mouse IgG (1:5000, Millipore). The blots were treated with enhanced chemiluminescence solution and exposed in gel imaging system (Bio-Rad).

Antibody-dependent Cellular Cytotoxicity

CytoTox 96 Nonradioactive Cytotoxicity assay (Promega, Madison, WI) was done based on the colorimetric detection of lactate dehydrogenase (LDH) released from the target cells K562, MDA-MB-435, or B16F10. HEK293 cells were used as control. Lymphocytes isolated from heparinized venous blood collected from a healthy volunteer served as the effector cells. Firstly, 5×10^3 K562, MDA-MB-435, B16F10, or HEK293 cells were cocultured with various amounts of the lymphocytes with or without the fusion protein at 37°C for 5 hours. Subsequently, 50 μ L of the supernatants were assayed for LDH activity following the manufacturer's protocol. Finally, controls for spontaneous LDH released in effector and target cells, as well as target maximum release, were prepared. The percentage of cytotoxicity was then calculated with the formula: % cytotoxicity = (experimental - effector spontaneous - target spontaneous) / (target maximum - target spontaneous) \times 100. MICA and scFv were used as controls.

Cytokine Production

Activated NK cells produce the cytokines interferon- γ (IFN- γ) and tumour necroses factor- α (TNF- α), therefore, the ability of the fusion protein to engage NKG2D-expressing effector cells was evaluated by its ability to induce NK cells to produce IFN- γ and TNF- α . Firstly,

NK92 and NK92^{shRNA} cells were respectively cocultured with MDA-MB-435 cells at a ratio 10:1 (effector:target), with or without the fusion protein of concentration 10 µg/mL or 50 µg/mL. After the incubation, the samples were fixed and permeabilized by Inside Stain Kit (MiltenyiBiotec, Germany). They were subsequently stained by intracellular antibody of TNF-α or IFN-γ (MiltenyiBiotec, Germany). Finally, the stained cells were analyzed by flow cytometry assay.

Statistical Analysis

Transwell and wound healing experiment were independently performed at least 3 times. The data of the study were analyzed using Excel and SPSS 17.0 software. Results are presented as the mean ± SD from at least 3 independent experiments. The *t* test was used to compare the inhibitory rates of different samples in MTT assay, transwell invasion assay. A *P*-value < 0.05 was considered statistically significant. All figures were generated with GraphPad Prism 5 software program.

RESULTS

Construction and Expression of the Fusion Protein

The scFv-MICA was made by joining ant-VEGFR2 scFv to the extracellular domain of MICA. A flexible linker (G₄S) was inserted between scFv and MICA to allow flexible interactions among scFv-MICA, VEGFR2, and NKG2D. The structure of scFv-MICA is shown in Figure 1. More importantly, the fusion protein is devoid of Fc fragment, therefore, binding of scFv-MICA to FcR-positive cells such as macrophages, B cells, neutrophils, and dendritic cells through the Fc fragment is eliminated, leading to less nontumor-associated NK activation. His-tag was directly added to the C-terminus of MICA to facilitate purification. In addition, as presented in Figures 1E and F, the scFv-MICA was expressed mainly as monomeric with molecular size 70 kD, which was in line with the expected size.

The Fusion Protein Binds to Both VEGFR2 (KDR) and NKG2D

To determine whether the fusion protein had preserved the binding affinity and specificity of the parental anti-VEGFR2 scFv and the MICA moiety, enzyme-linked immunosorbent assay, and Western blotting assays were carried out. As shown in Figure 2, the fusion protein was able to bind to both KDR3 and NKG2D in a dose-

dependent manner. The binding ability of the fusion protein was further confirmed by the binding kinetics studies, where equilibrium constant (K_D) 3.95 × 10⁻⁸M against KDR3 and 6.13 × 10⁻⁷M against NKG2D (Figs. 2E, F) were recorded. Furthermore, the fusion protein demonstrated

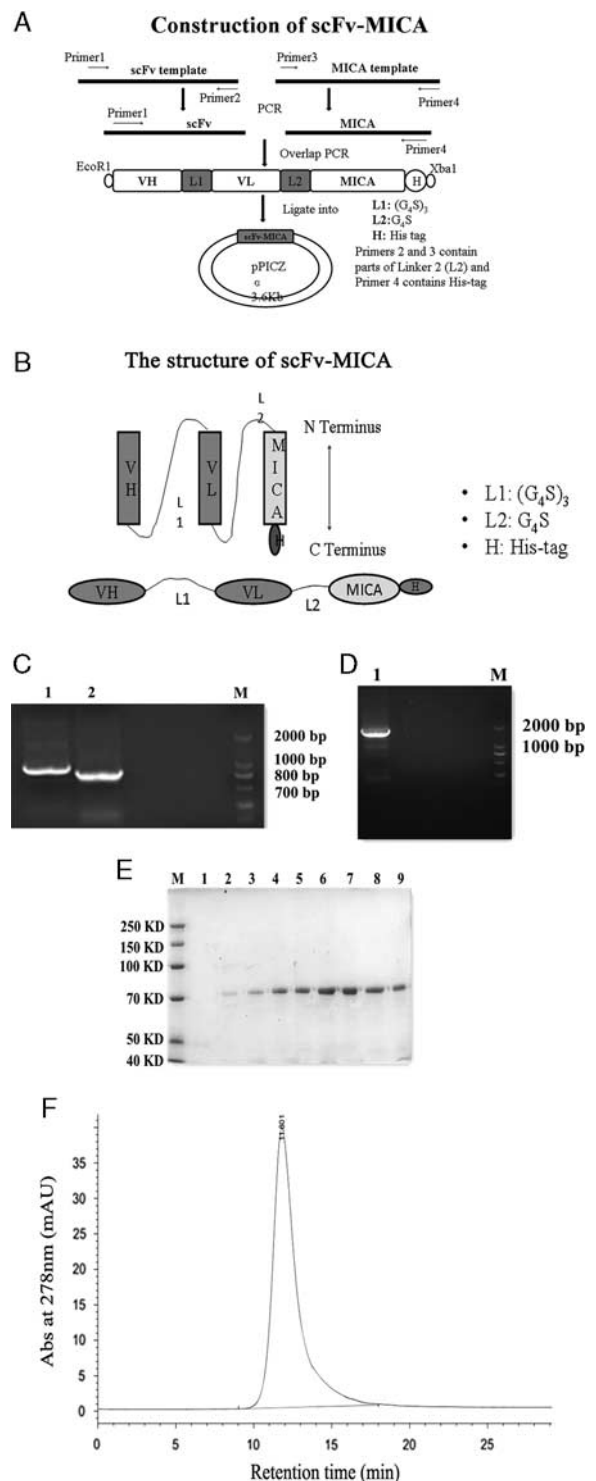


FIGURE 1. A, Schematic diagram of the construction of the recombinant vector (pPICZα-scFv-MICA). L₁: linker1 [(G₄S)₃], L₂: linker2(G₄S); *EcoR1* and *Xba1*: Restriction sites. B, Schematic diagram of the structure of fusion protein. C, PCR of MICA and scFv. Lane 1: MICA (828 bp); Lane 2: scFv (735 bp); M: Marker. D, PCR of scFv-MICA. Lane 1: scFv-MICA (1596 bp); M: Marker. E, Coomassie-stained SDS-PAGE analysis of the purified fusion protein (70 kD). M: Marker; Lane 1–9: Different elutions of the purified fusion protein. F, Chromatogram of size exclusion chromatographic analysis of the fusion protein. PCR indicates polymerase chain reaction; scFv-MICA, single-chain variable fragment-major histocompatibility complex class I-related chain A; SDS-PAGE, sodium dodecyl sulfate polyacrylamide gel electrophoresis.

binding specificity to native VEGFR2 and NKG2D expressed on HUVECs and U937 cells, respectively (Fig. 3). NK92 cells transiently transfected with lentiviral plasmids pLVX-shRNA-NKG2D, and untreated NK92 cells were used as control. As presented in Figure 3E, the fusion protein demonstrated significant binding affinity to the untreated NK92 cells, however, its binding affinity to NK92 cells transiently transfected with lentiviral plasmids pLVX-shRNA-NKG2D was relatively low.

ScFv-MICA Inhibits HUVEC Sproliferation, Migration, and Invasion

The ability of the fusion protein to restrain the proliferation and migration of HUVEC cells was determined by cell proliferation assay¹⁷ and wound healing assay.¹⁸ As shown in Figures 4A and B, the fusion protein significantly restrained the proliferation of the HUVEC cells in a time-dependent and dose-dependent manner, with respective IC₅₀ values ~333.186, ~248.198, and ~186.816 nM being recorded at 24, 48, and 72 hours. As presented in Figures 4C and D, the width of the gaps of the negative control (PBS and MICA) treated groups narrowed faster from 0 to 24 hours compared to the fusion protein and scFv-treated groups.

As demonstrated in Figures 5A and B, the fusion protein dose-dependently restrained HUVECs invasion.¹⁹ In addition, the inhibitory potential of the fusion protein on tube formation by HUVECs was evaluated by tube formation assay.²⁰ As shown in Figures 5C and D, the fusion protein dose dependently blocked tube formation by HUVECs.

Western Blot Analysis

VEGFR2 moderates endothelial cells proliferation and migration by regulating the expression of P38 MAPK. Therefore to investigate the inhibitory effects of the fusion protein on HUVECs proliferation and migration, the inhibitory effect of the fusion protein on the phosphorylation of P38 MAPK was examined. As shown in Figure 5E, the fusion protein dose-dependently inhibited P38 MAPK phosphorylation, suggesting that the fusion protein could restrain cell proliferation and migration of endothelial cells. In addition, the effect of the fusion protein on the activation of AKT downstream was evaluated, and as shown in Figure 5E, the fusion protein dose dependently inhibited the phosphorylation of AKT signaling, further

confirming the antiangiogenic potential of the fusion protein.

ScFv-MICA Induces Cell-mediated Cytotoxicity in VEGFR2-expressing Cancer Cells

To investigate whether the fusion protein induces cell-mediated cytotoxicity, we examined cell-mediated cytotoxicity in VEGFR2-expressing tumor cells in the presence of NKG2D-expressing effector cells. As shown in Figure 6, in

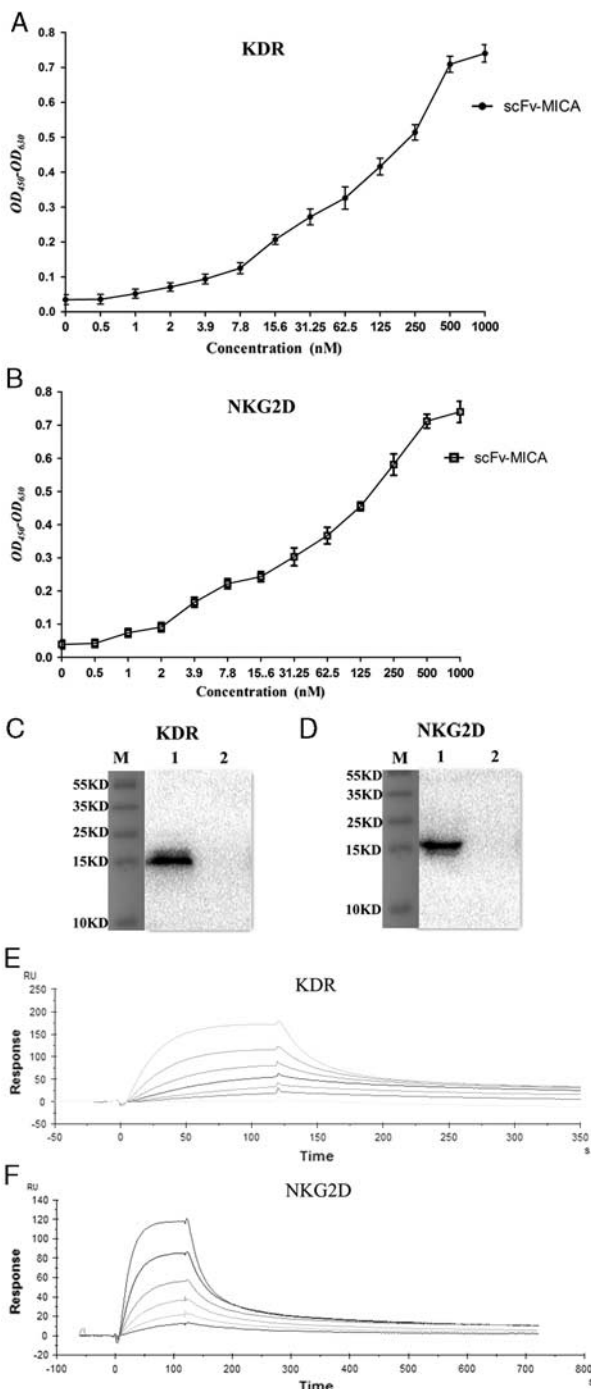


FIGURE 2. A and B, The fusion protein binds to recombinant NKG2D and KDR3 by enzyme-linked immunosorbent assay. C, The fusion protein binds to recombinant KDR3 (15 kD) by immunoblotting. Lane 1: fusion protein binds to KDR3 (binding blot present); Lane 2: The fusion protein did not bind to the control sample scFv (28 kD), (binding blot absent). D, The fusion protein binds to recombinant NKG2D (16 kD) by immunoblotting. Lane 1: fusion protein binds to NKG2D (absence of binding blot); Lane 2: The fusion protein demonstrated no binding ability to the control sample scFv, (absence of binding blot). E, SPR sensorgrams of the binding kinetics of the fusion protein against the recombinant KDR3. $k_a = 4.26 \times 10^6/\text{MS}$, $k_d = 261/\text{S}$, and $K_D = 6.13 \times 10^{-7}\text{M}$. F, SPR sensorgrams of the binding kinetics of the fusion protein against the recombinant NKG2D. $k_a = 6.77 \times 10^9/\text{MS}$, $k_d = 267.4/\text{S}$, and $K_D = 3.95 \times 10^{-8}\text{M}$. KDR indicates kinase insert domain-containing receptor; NKG2D, natural killer group 2 member D.

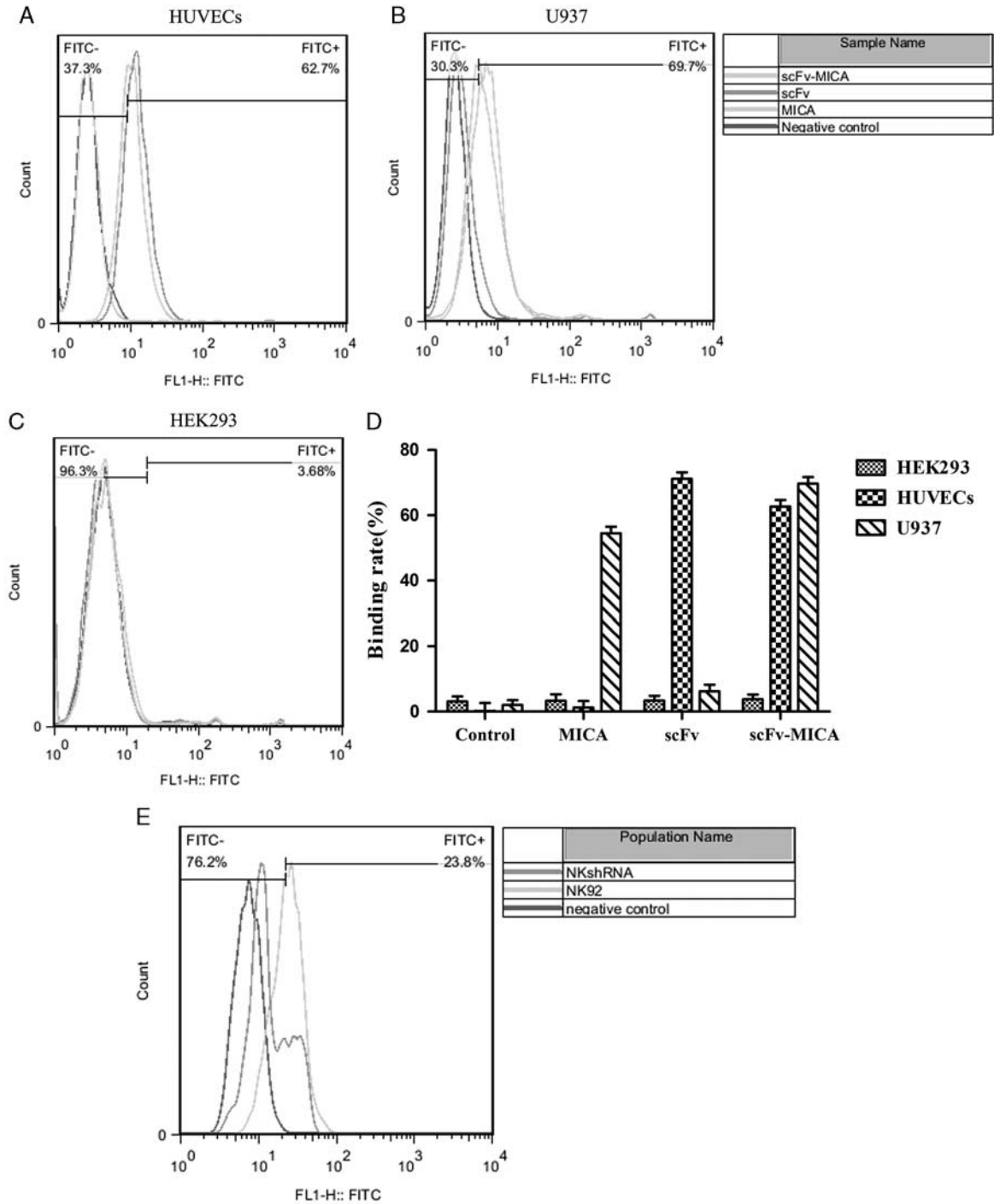


FIGURE 3. A, The fusion protein binds to VEGFR2-expressing human umbilical vein endothelial cells (HUVECs), with rate ~62.7%. B, Fusion protein binds to NKG2D-expressing U937 cells with rate ~69.7%. C, The fusion protein, MICA, scFv, and PBS demonstrated no significant binding to the control cell line HEK293. D, Quantitative analysis of the flow cytometric assays revealed that the fusion protein binds to NKG2D-expressing U937 cells and VEGFR2-expressing HUVEC cells but not the control cell line HEK293. E, The fusion protein demonstrated relatively significant binding affinity to NKG2D-expressing NK92 with rate ~76.2% but not NK92 cells transiently transfected with lentiviral plasmids pLVX-shRNA-NKG2D. NKG2D indicates natural killer group 2 member D; scFv-MICA, single-chain variable fragment-major histocompatibility complex class I-related chain A.

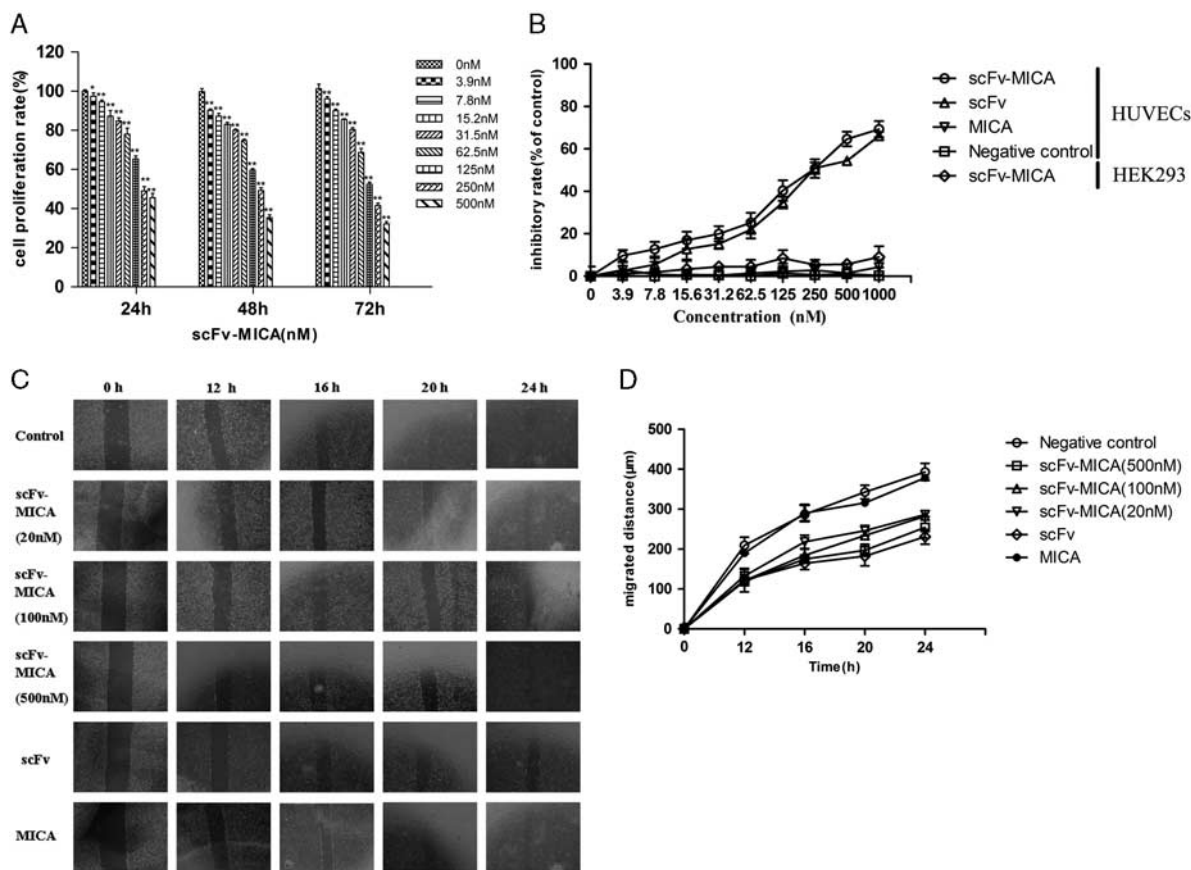


FIGURE 4. A, The fusion protein demonstrated significant restraining effect on the proliferation of HUVEC cells in dose-dependent and time-dependent manner. B, The fusion protein blocked the proliferation of HUVEC cells in a dose-dependent and time-dependent manner. However, it exhibited no significant inhibition on VEGFR2-negative HEK293 cells. (Values represent means \pm SD, n = 3, * P < 0.05, ** P < 0.01 vs. untreated control). C, Photomicrographs of wound healing assay showing that, the fusion protein dose-dependently restrained the migration of HUVECs. D, Quantitative analysis of the wound healing assay which revealed that, the fusion protein treated HUVECs migrated more slowly after wounding. HUVEC indicates human umbilical vein endothelial cells; scFv-MICA, single-chain variable fragment-major histocompatibility complex class I-related chain A.

the presence of the effector cells (lymphocytes), the fusion protein significantly induced cell-mediated cytotoxicity in K562, MDA-MB-435, and B16F10 cancer cells, which increased with increasing E/T (effector/target) ratio. On the contrary, scFv and MICA could not significantly induce cell-mediated cytotoxicity in MDA-MB-435 and B16F10, but seemed to have successfully induced cytotoxicity in K562 cell (Fig. 6A). It is interesting to note that the effector cells also demonstrated some level cytotoxicity in the K562 cells in the absence of the fusion protein, MICA and scFv (Fig. 6A), which implied that, MICA and scFv could not have played any active role in the cytotoxicity of the K562 cells. As anticipated, the fusion protein did not induce cytotoxicity in the control cell line HEK293 (Fig. 6D), demonstrating its specificity.

Fusion Protein Activates NK Cells to Produce TNF- α and IFN- γ

Production of TNF- α and IFN- γ by NK92 cells was examined, when cocultured with tumor cell MDA-MB-435 in the presence or absence of the fusion protein. As shown in Figures 6E and F, the NK92 cells produced significant

amounts of TNF- α and IFN- γ in the presence of both MDA-MB-435 and the fusion protein, which was not the case when the NK92 cells were cocultured with MDA-MB-435 cells in the absence of the fusion protein. In addition, as presented in Figures 6G and H, production of TNF- α and IFN- γ were relative low when NK92^{shRNA} cells were cocultured with MDA-MB-435 cells in the presence of the fusion protein. These data indicate that the fusion protein engages the NK cells to functionally recognize VEGFR2-expressing tumor cells.

DISCUSSION

Antibody therapy is now the preferred strategy in modern medicine for the treatment of cancers. However, it has its own functional limitations, which can be attributed to the large molecular size (150 kD) and possibly the presence of Fc fragment which can easily be involved in nonspecific binding.^{3,6} The hypothesis was that, the efficacy of such useful antibodies can be improved, if the molecular size was reduced to an acceptable size for easy absorption, and the Fc fragment was replaced with more functionally specific moiety through

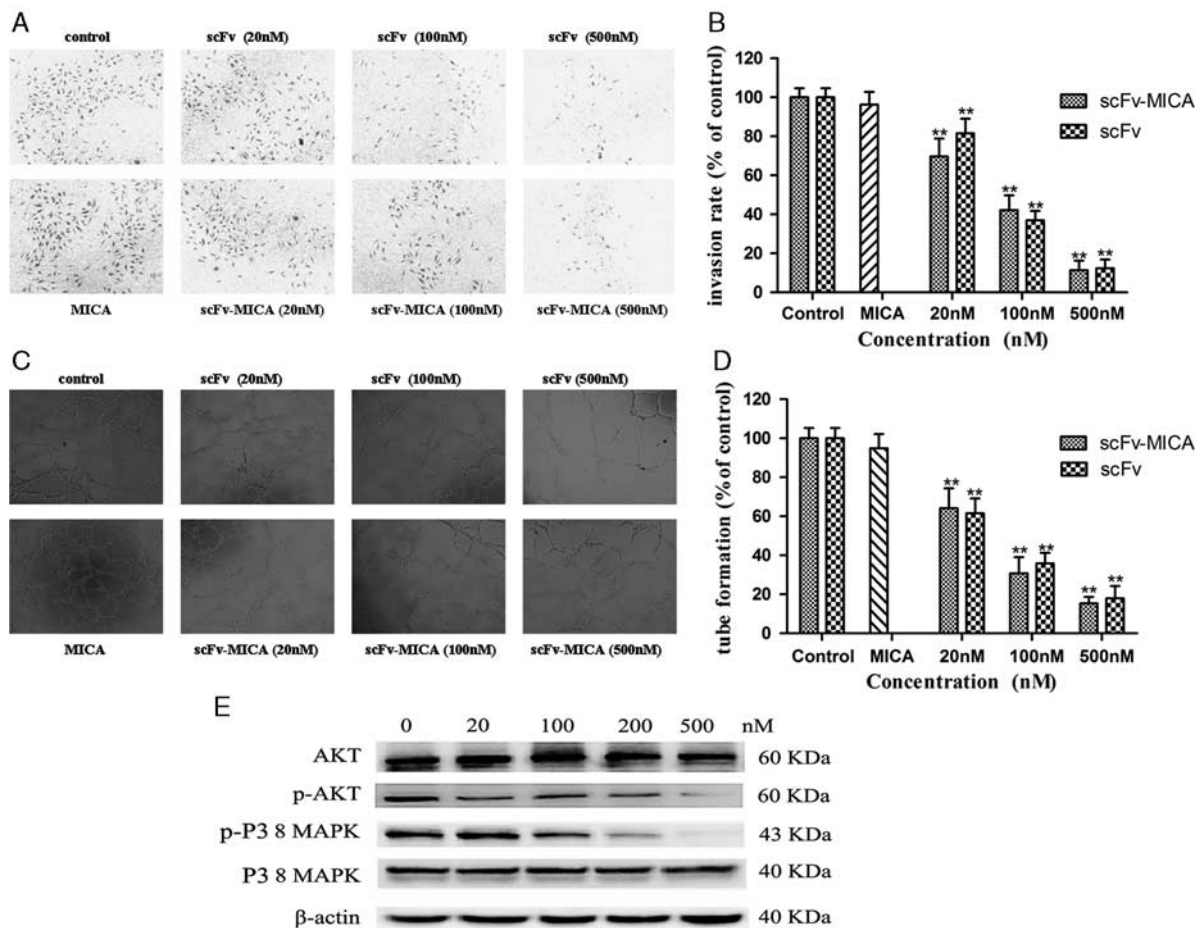


FIGURE 5. A, Photomicrographs of transwell invasion assay showing that, the fusion protein could potentially inhibit invasion by HUVEC. B, Quantitative analysis of the transwell invasion assay indicated that, the fusion protein suppressed the invasion of HUVECs in a dose-dependent manner and the data were presented as the mean \pm SD, $n=5$, $**P<0.01$, vs. untreated group. C, Photomicrographs showing the significant effects of the fusion protein on HUVECs tube formation. D, Quantitative analysis of the tube formation assay indicated that the fusion protein significantly restrained tube formation by human umbilical vein endothelial cells in a dose-dependent manner (data were presented as the mean \pm SD, $n=5$, $**P 0.01$ vs. untreated group). E, Western Blot analysis of the inhibition of the phosphorylation of P38 mitogen-activated protein kinases and protein kinase B by the fusion protein. AKT indicates protein kinase B; MAPK, mitogen-activated protein kinases; scFv-MICA; single-chain variable fragment-major histocompatibility complex class I-related chain A. ** indicates that there is a significant difference between the date of different groups.

molecular engineering. We previously developed a novel anti-VEGFR2 scFv,⁵ but due to its short half-life as a result of smaller molecular size (30kD), coupled with the fact that it lacked Fc fragment for effector cell recognition, further engineering was needed to improve its efficacy. It was therefore necessary to incorporate robust avidity and effector recognition function in our anti-VEGFR2 scFv. A novel fusion protein scFv-MICA was therefore created by joining the extracellular domain of MICA to our anti-VEGFR2 scFv, to address these shortcomings. Through immunosurveillance, the immune system is able to recognize and eliminate stressed cells through stress proteins such as MICA which is expressed on these diseased cells. Contrary to other stressed cells, most cancer cells are capable of shedding of MICA and therefore are able to escape immunosurveillance.⁷ The fusion protein as an immunotherapeutic agent was therefore engineered to facilitating the recognition and elimination of cancer cells by effector cells by binding cancer cells via scFv/VEGFR2 pathway and the effector cells via MICA/NKG2D pathway. The

fusion protein is therefore a potential immunotherapeutic agent which can be developed further and used for cancer therapy.

The new fusion protein has shown that it is capable of binding to both antigen VEGFR2 and receptor NKG2D, demonstrating that, it is made up of the correct moieties, and that each moiety had retained its functional property. Furthermore, Size exclusion chromatographic analysis of the fusion protein showed that, the fusion protein was successfully expressed as monomeric, with >90% purity. This implied that, nonspecific polyclonal activation, usually associated with protein aggregates and recombinant antibodies may be minimized. In addition, the fusion protein demonstrated that it could inhibit proliferation, wound healing, transwell invasion, and tube formation of the HUVECs. These data were corroborated with western blot analysis where the fusion protein significantly inhibited the phosphorylation of AKT and P38 MAPK which are significant markers of angiogenesis in cancers.

Furthermore, the fusion protein induced cell-mediated cytotoxicity in VEGFR2-expressing tumor cells MDA-MB-435 and B16F10 in the presence of effector cells. The data indicated that, the fusion protein could engage both effector and tumor cells simultaneously through the MICA and scFv moieties respectively. The moieties of the fusion protein MICA and scFv could not induce significant cytotoxicity in the tumor cells in their individual capacities. Although, some level susceptibility seemed to have been recorded in K562 as a result of MICA and scFv moieties (Fig. 6A), evidence however points to the fact that, it is due the effector cells. It has been reported elsewhere that K562 is susceptible to NK cells,²¹ therefore the cell-mediated cytotoxicity in the K562 cells can be attributed to the lymphocytes.

Activated NK cells produce IFN- γ and TNF- α , which synergistically enhance NK cell cytotoxicity through NF- κ B-dependent up-regulation of ICAM-1 expression in target cells.²² The fusion protein induced significant production of IFN- γ and TNF- α , confirming its ability to induce cell-mediated cytotoxicity in VEGFR2 carrying tumor cells. These data confirmed that, the fusion protein engaged both VEGFR2-expressing tumor cells and the NKG2D-expressing effector cells simultaneously and it is specific in its function.

Fusing MICA to the parental scFv has significantly improved its efficacy. Besides its core antiangiogenic efficacy, the improved scFv (fusion protein) was able to induce cell-mediated cytotoxicity in VEGFR2-expressing tumor cells. In addition, fusing MICA to the scFv resulted in an increase in molecular size from (scFv) 28kD to (scFv-MICA) 70 kD, which may prolong the serum half-life and for that matter, improve its efficacy. Another advantage the fusion protein has over traditional mAb is that, it is relatively smaller than mAbs. Cancer therapeutic mAbs such as

ramucirumab (anti-VEGFR2) largely remain in the blood, and >20% of the administered dose gets to the cancer cells, due to the large molecular size (150kD), characterized by low absorption rate.^{3,23} In the light of these facts, further studies are on going to evaluate the safety profile and efficacy of the fusion protein in vivo.

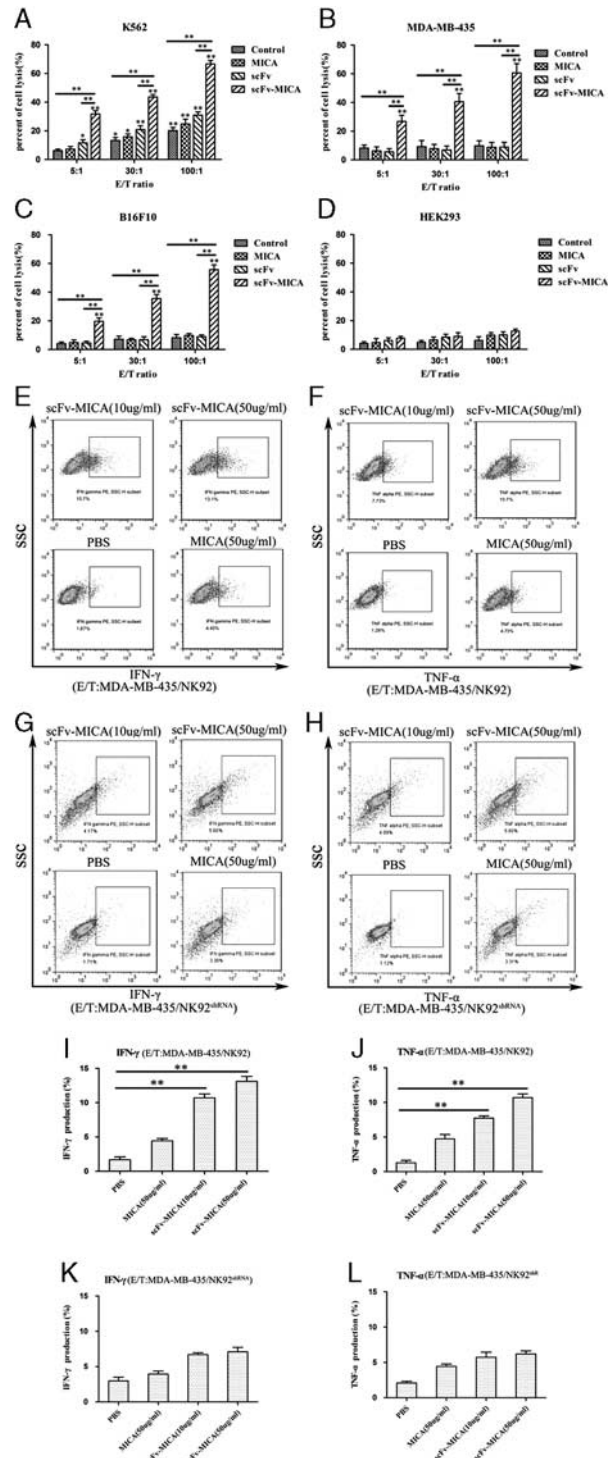


FIGURE 6. A, The fusion protein induced significant cell-mediated cytotoxicity in K562 cells in the presence of lymphocytes (data were presented as the mean \pm SD, n=5, * P <0.05, ** P <0.01 vs. untreated group). B, The fusion protein significantly activated cell-mediated cytotoxicity in VEGFR2-expressing MDA-MB-435 cells when cocultured with lymphocytes (data were presented as the mean \pm SD, n=5, * P <0.05, ** P <0.01 vs. untreated group). C, The fusion protein was able to induced significant cytotoxicity in VEGFR2-expressing B16F10 cells in the presence of lymphocytes (data are presented as the mean \pm SD, n=5, * P <0.05, ** P <0.01 vs. untreated group). D, As anticipated, the fusion protein could not induce significant cell-mediated cytotoxicity in VEGFR2-negative HEK293 cells (data were presented as the mean \pm SD, n=5, * P <0.05, ** P <0.01 vs. untreated group). E and F, Significant production of TNF- α (E) and IFN- γ (F) by NK92 cells, cocultured with VEGFR2-expressing MDA-MB-435 cells in the presence of fusion protein was detected by flow cytometry assay. G and H, Relatively low production of TNF- α (G) and IFN- γ (H) was associated with NK92^{shRNA} cocultured with MDA-MB-435 cells in the presence of the fusion protein. I-L, Quantitative analysis of the production of TNF- α (I) and IFN- γ (J) by NK92 cells and TNF- α (K) and IFN- γ (L) by NK92^{shRNA} cocultured respectively with the fusion protein. These data indicated that the fusion protein engaged the NK29 cells (data were presented as the mean \pm SD, n=5, * P <0.05, ** P <0.01 vs. untreated group). E/T indicates effector/target; scFv-MICA, single-chain variable fragment-major histocompatibility complex class I-related chain A.

In conclusion, the generated novel fusion protein (scFv-MICA) has demonstrated potent antiangiogenic and anti-neoplastic activities. Furthermore, it has shown that, it can induce cell-mediated cytotoxicity in VEGFR2-expressing tumor cells by engaging NKG2D-expressing effector cells. In addition, the fusion protein with relatively smaller molecular size (70 kD) may have better antitumor potential and minimal toxicity in vivo compared with the full IgG1 with larger molecular size 150 kD. The fusion protein targeting therefore provides the means to engage NKG2D-expressing effector cells against VEGFR2-expressing tumor cells. Hence, this cancer treatment strategy can be explored further to develop potent anticancer agent.

CONFLICTS OF INTEREST/FINANCIAL DISCLOSURES

This project was supported by the National Natural Science Foundation of China (NSFC81072561, NSFC81102364, and NSFC81273425). The Project Program of State Key Laboratory of Natural Medicines (China Pharmaceutical University, JKGP201101). A project funded by the Priority Academic Program Development of Jiangsu Higher Education Institutions. Graduate Student Innovation Project Funded by Huahai Pharmaceutical Co. (CX13S-009HH).

All authors have declared that there are no financial conflicts of interest with regard to this work.

REFERENCES

- Papadopoulos N, Martin J, Ruan Q, et al. Binding and neutralization of vascular endothelial growth factor (VEGF) and related ligands by VEGF Trap, ranibizumab and bevacizumab. *Angiogenesis*. 2012;15:171–185.
- Fuchs CS, Tomasek J, Yong CJ, et al. Ramucirumab monotherapy for previously treated advanced gastric or gastroesophageal junction adenocarcinoma (REGARD): an international, randomised, multicentre, placebo-controlled, phase 3 trial. *Lancet*. 2014;383:31–39.
- Chames P, Van Regenmortel M, Weiss E, et al. Therapeutic antibodies: successes, limitations and hopes for the future [J]. *Br J Pharmacol*. 2009;157:220–233.
- Xie W, Li D, Zhang J, et al. Generation and characterization of a novel human IgG1 antibody against vascular endothelial growth factor receptor 2. *Cancer Immunol Immunother*. 2014; 63:877–888.
- Zhang J, Li H, Wang X, et al. Phage-derived fully human antibody scfv fragment directed against human vascular endothelial growth factor receptor 2 blocked its interaction with VEGF. *Biotechnol Prog*. 2012;28:1–10.
- Zhang T, Sentman CL. Cancer immunotherapy using a bispecific NK receptor- fusion protein that engages both T cells and tumor cells. *Cancer Res*. 2011;71:2066–2076.
- Jamieson AM, Diefenbach A, McMahon CW, et al. The role of the NKG2D immunoreceptor in immune cell activation and natural killing. *Immunity*. 2002;17:19–29.
- Raulet DH. Roles of the NKG2D immunoreceptor and its ligands. *Nature Rev Immunol*. 2003;3:781–790.
- Le Bert N, Gasser S. Advances in NKG2D ligand recognition and responses by NK cells. *Immunology and Cell Biology*. 2014;92:230–236.
- Roberts AI, Lee L, Schwarz E, et al. NKG2D receptors induced by IL-15 costimulate CD28-negative effector CTL in the tissue microenvironment. *J Immunol*. 2001;167: 5527–5530.
- Yang F, Tang X, Riquelme E, et al. Increased VEGFR-2 gene copy is associated with chemoresistance and shorter survival in patients with non-small-cell lung carcinoma who receive adjuvant chemotherapy. *Cancer Res*. 2011;71:5512–5521.
- Lee TH, Seng S, Sekine M, et al. Vascular endothelial growth factor mediates intracrine survival in human breast carcinoma cells through internally expressed VEGFR1/FLT1. *PLoS Med*. 2007;4:e186.
- Silva SR, Bowen KA, Rychahou PG, et al. VEGFR-2 expression in carcinoid cancer cells and its role in tumor growth and metastasis. *Int J Cancer*. 2011;128:1045–1056.
- Duff SE, Jeziorska M, Rosa DD, et al. Vascular endothelial growth factors and receptors in colorectal cancer: implications for anti-angiogenic therapy. *Eur J Cancer*. 2006;42: 112–117.
- Auguste P, Lemiere S, Larrieu-Lahargue F, et al. Molecular mechanisms of tumor vascularization. *Crit Rev Oncol Hematol*. 2005;54:53–61.
- Zhao X, Acheampong DO, Wang Y, et al. Efficient in vitro refolding and characterization of major histocompatibility complex class I-related chain molecules a (MICA) and natural killer group 2 member D (NKG2D) expressed in *E. coli*. *Protein Pept Lett*. 2015;22:460–469.
- Shibuya M, Claesson-Welsh L. Signal transduction by VEGF receptors in regulation of angiogenesis and lymphangiogenesis. *Exp Cell Res*. 2006;312:549–560.
- Wahl O, Oswald M, Tretzel L, et al. Inhibition of tumor angiogenesis by antibodies, synthetic small molecules and natural products. *Curr Med Chem*. 2011;18:3136–3155.
- Ferrara N, Kerbel RS. Angiogenesis as a therapeutic target. *Nature*. 2005;438:967–974.
- Saharinen P, Eklund L, Pulkki K, et al. VegF and angiopoietin signaling in tumor angiogenesis and metastasis. *Trends Mol Med*. 2011;17:347–362.
- Lozzio BB, Lozzio CB. Properties and usefulness of the original K-562 human myelogenous leukemia cell line. *Leukemia Research*. 1979;3:363–370.
- Wang R, Jaw JJ, Stutzman CN, et al. Natural killer cell-produced IFN- γ and TNF- α induce target cell cytotoxicity through up-regulation of ICAM-1. *J Leukoc Biol*. 2012;91: 299–309.
- Beckman RA, Weiner LM, Davis HM. Antibody constructs in cancer therapy: protein engineering strategies to improve exposure in solid tumors. *Cancer*. 2007;109:170–179.